NJC

Accepted Manuscript

ROYAL SOCIETY
OF CHEMISTRY

www.rsc.org/njc

Revised

Fabrication and characterization of novel highly transparent and organo-soluble poly(ether imide)s thin film for gas separation

Mohammad Dinari [*] **, Hashem Ahmadizadegan and Parvin Asadi**

Organic Polymer Chemistry Research Laboratory, Department of Chemistry, Isfahan University of Technology, Isfahan, 84156-83111, I. R. Iran.

---

[*] Corresponding author. Tel.; +98-31-3391-3270; FAX: +98-31-3391-2350.

E-mail address: dinari@cc.iut.ac.ir, mdinary@gmail.com (M. Dinari).

Abstract

The novel diamine with ether and phenyl linkages was prepared in two steps by the nucleophilic substitution reaction of 2-(2-hydroxy-5-methylphenylsulfinyl)-4-methylphenol and 1-chloro-4-nitrobenzene in *N*,*N′*-dimethylacetamide, followed by reduction with hydrazine monohydrate and a Pd/C in ethanol. Four series of solution-processable aromatic poly(ether imide)s (PEI)s were prepared from new synthesized diamine and various dianhydride *via* one-step high-temperature solution polymerization. The diamine monomer and PEIs were characterized by elemental analyses, Fourier transform infrared spectra and nuclear magnetic resonance spectroscopy. The inherent viscosities of the obtained poly (amic-acid) (PAA) were ranged from 1.09 to 1.93 dL/g at a concentration of 0.5 g/dL in *N*,*N′*-dimethylacetamide at 30 ^{o}C. All the obtained polymers were readily soluble in polar solvents and showed useful levels of thermal stability associated with high glass-transition temperatures (T_g, 279-303 ^{o}C) and high char yields (higher than 62 % at 800 ^{o}C in nitrogen). Flexible and transparent films can be obtained easily by solution casting. The cast films exhibited high optical transparency and almost no color, with a UV-Vis absorption edge of 368-382 nm. These films also showed excellent mechanical properties with the tensile strengths of 118-154 MPa and elongations at breakage of 11-15%. The combination of excellent solubility, film quality, and thermal stability makes these PEIs as potential candidates for high-performance gas separation membrane applications by solution-casting processes. Permeability measurements were made for O_2, H_2, CO_2 and CH_4 at 35 °C.

Keywords: Diamine with ether linkages; Poly(ether imide)s; Thermal stability; Gas separation

1. Introduction

Polymers that can be processed from solution to form microporous solids are of growing interest for use as highly permeable membranes for gas separations. Polymer-based gas separation membranes are expected to contribute in numbers of considerable environmental and energy technologies including gas purification and capture.[1-3] The main parameter for the design and preparation of high-performance gas separation membranes are high permeability and good selectivity.[4] Conversely, there is an inherent trade-off of gas pairs between permeability and selectivity for all the gas separation polymer membranes, which was quantified in 1991 and 2008 by Robeson.[5,6] The upper bound was identified on plots of double logarithmic plots of selectivity against permeability for a wide range of gas pairs using a comprehensive list of existing polymer permeabilities.

Aromatic polyimides (PIs) are known as a class of high performance materials because of their outstanding resistance to solvent, natural pyrolysis and thermo-oxidative decomposition as well as mechanical strength and excellent electrical properties. So, these polymers are generally used in the fields of adhesives, sealants, electrical packaging, interlayer dielectrics, as high temperature insulators for aircraft wire coatings, as membranes for gas separation and as materials in flexible printed circuits materials.[7-12] However, for numerous applications, these polymers require having high thermal stability, good film-forming ability, enough organo-solubility and improved chemical resistance. But, wholly aromatic PIs, due to their high melting or glass-transition temperatures (T_g's), their limited solubility in most organic solvents and deficiencies transparency, do not present the optimum properties for many applications. Inherent macromolecular stiffness and strong interchain forces are usually offered to give details these processing difficulties. In fact, the heterocyclic imide units provide the polymer chain rigidity and impart high interchain interactions.[11,13,14] To overcome these limitations, synthetic suggests have been centered on increasing their solubility in organic solvents without sacrificing the above mentioned outstanding properties.[12] New synthetic techniques have been focused on improving processability and solubility through the synthesis of new diamine or dianhydride monomers. Attempts in this field include introduction of flexible linkage, bulky substituents, and structurally unsymmetrical segments into the polymer backbone which leads to an increase in processability, the reduction in crystallinity and reduction of intermolecular interactions such as chain packing, charge transfer complex and electronic polarization interactions.[15-18] The synthesis of newly aromatic monomers such as heteroaromatic diamines or dianhydrides plays vital role in prepares of advanced PI materials. Commonly, the novel class of heteroaromatic diamines, dianhydrides or other monomers can help for the thermal stability, chemical resistance and retention of mechanical property of the resultant polymer. So, the heteroaromatic structures in the main chain of a polymer make positive properties to it.[8] Additionally, the standard aromatic PIs showed yellow to brown in colors due to the intra- and inter-molecular charge transfer interactions between the alternating electron-donor (diamine) and electron-acceptor (dianhydride) moieties.[19-21] Therefore, considerable efforts have been made in recent years to develop highly optical transparent, low-*k* and low-*n* aromatic PIs with good processability by using of polyisoimides as the polyimide precursor[22], or by introducing of flexible linkages, fluorinated substituents, unsymmetrical units or bulky pendent groups into the polymer backbones.[23-25]

Aromatic ether linkages are the most popular and flexible linkages inserted in polymer backbones make them with extensively lower energy of internal rotation. Such a structural modification results in a lower T_g and crystalline melting temperature as well as a significant enhancement in the toughness, solubility and process characteristics without greatly sacrificing thermal stability.[26-30]

In this article, a new kind of a high-purity ether-containing diamine monomer was synthesized by the nucleophilic substitution reaction of 2-(2-hydroxy-5-methylphenylsulfinyl)-4-methylphenol and 1-chloro-4-nitrobenzene in *N*,*N′*-dimethylacetamide (DMAc), followed by reduction with hydrazine monohydrate and a Pd/C in ethanol. A new series of aromatic poly(ether imide)s (PEI)s were synthesis by the reaction of resulting diamine monomer with four different dianhydride such as 4,4'-(hexafluoroisopropylidene) diphthalic anhydride (a or 6FDA), 4,4′-benzophenone tetracarboxylicdianhydride (b or BTDA), 4,4'-oxydiphthalic dianhydride (c or ODPA) and 3,3',4,4′-diphenylsulfone tetracarboxylic dianhydride (d or DSDA). The obtained diamine and related intermediates as well as PEIs were characterized by elemental analyses, Fourier transform infrared (FT-IR), proton nuclear magnetic resonance (^{1}HNMR) spectroscopy, X-ray diffraction (XRD), thermogravimetry analysis (TGA), and differential scanning calorimetry (DSC) techniques. The effect of the flexible linkages on the tensile stress-strain of PEI films was investigated. Also the permeability measurements were made for O_2, H_2, CO_2 and CH_4 at 35 °C.

2. Experimental

2.1. Materials

Commercial aromatic dianhydrides were purchased from Aldrich Chemical Co. and was purified by recrystallization from acetic anhydride. BTDA was dried at 120 °C overnight before using. Triethylamine were obtained from Aldrich Chemical Co. *N*-methyl-2-pyrrolidone (NMP), *N*,*N*-dimethylformamide (DMF) and DMAc were dried over barium oxide, followed by fractional distillation. Other chemicals were purchased from Merck Chemical Co.

2.5. Equipments

The FT-IR spectra were taken at room temperature with a resolution of 4 cm^{-1} using 400 D IR spectrophotometer (Japan). Band intensities are assigned as weak (w), medium (m), strong (s), and broad (br). NMR spectra were recorded at room temperature using Bruker (Germany) Avance 500 instrument at 500 MHz for ^{1}H-NMR and at 125 MHz for ^{13}C-NMR. Solvent used for analysis was deutrated dimethyl sulfoxide (DMSO-d_6). Proton resonances are designated as singlet (s), doublet (d), and multiplet (m). Elemental analyses were run in an elemental analyses system GmbH, Germany. Inherent viscosities were determined with a Cannon-Fenske Routine Viscometer (Germany) at concentration of 0.5 g/dL at 30 ^{o}C in DMAc. Gel permeation chromatography (GPC) was performed with a Waters instrument (Waters 2414) and tetrahydrofuran (THF) was used as eluent (flow rate 0.5 mL/min). Polystyrene was used as standard and RI detector was used to record the signal in GPC. TGA was performed with a Perkin Elmer. The samples heated in nitrogen atmosphere from 25 to 800 $^{\circ}$C at a heating rate of 20 °C/min. DSC analyses were performed on a Perkin Elmer Pyris 1 DSC at a scan rate of 20 °C/min in flowing nitrogen (35 cm^3/min). An X-ray diffractometer (Philips Xpert MPD, Germany), with Cu Kα radiation (λ = 1.540 Å) was employed to determine the structure of newly synthesized polymers. Bragg angles ranged from 10-80° at the speed of 0.05°/min. The operating current and voltage were maintained at 30 mA and 40 kV, respectively. The mechanical properties were measured on a Testometric Universal Testing Machine M 350/500 (UK), consistent by means of ASTM D 882 (standards). Tests were carried out through a cross-head speed of 12.5 mm/min until/to a deformation of 20% and then at a speed of 50 mm/min at break. The optical properties of polymers were studied with a JASCO V-750 (Tokyo, Japan) in the spectral range between 200 and 800 nm. The gas permeability of the polymer membranes with thickness around 30 μm was measured with a automated Diffusion Permeameter (DP-100-A) manufactured by porous materials Inc., USA, which consists of upstream and downstream parts separated by a membrane. Gases measured include O_2, N_2, CO_2, and CH_4. The permeation cell was placed in a thermostatically controlled housing for maintaining isothermal measurement conditions. The reproducibility of the measurements was checked from three independent measurements using the same membrane and it was better than ±5%.

2.3. Synthesis of diamine monomer

At first, in a 50-ml three-neck round-bottomed flask equipped with a stirring bar under nitrogen atmosphere, 2.00 g (7.63 mmol) of 2-(2-hydroxy-5-methylphenylsulfinyl)-4-methylphenol, 2.39 g (15.26 mmol) of 1-chloro-4-nitrobenzene, 2.14 g (15.55 mmol) of potassium carbonate, and 20 mL of DMAc was added. The solution was stirred at 125 °C for 5 h. After cooling to room temperature, the mixture was poured into 300 mL of methanol. The precipitate was dried at 70 ^{o}C under vacuum and the product was recrystallized from glacial acetic acid to give dinitro monomer in 90% yield; mp 215-219 °C. In the second step, a mixture of hydrazine monohydrate (3 mL), dinitro compound (2.00 g, 3.96mmol), a catalytic amount of 10% Pd/C (0.3 g), and ethanol (170 mL) was heated at the reflux temperature for 18h. In order to remove Pd/C, the reaction solution was filtered and purified by recrystallized from methanol and then it was dried in vacuum (80% yield; mp 171-175 °C).

FT-IR (KBr, cm^{-1}): 3447 (s), 3383 (s), 3133 (w), 3180 (w), 1555 (m), 1525 (m) 1529 (w), 1326 (w), 1147 (w), 832 (m), 773 (w).

^{1}H NMR (500 MHz, DMSO-d_6, ppm): 2.37 (s, 6H, CH), 4.59 (s, 4H, NH), 6.76-6.77 (d, 1H, Ar-H, J= 3.5), 6.98-6.98 (d, 1H, Ar-H, J= 4.5 Hz), 7.34-7.35 (d, 4H, Ar-H), 7.63 (s, 2H, Ar-H).

^{13}C NMR (125 MHz, DMSO-d_6), δ (ppm): 39.55 (CH_3), 109.11 (Ar), 110.09 (Ar), 115.61 (Ar), 118.66 (Ar), 122.20 (Ar), 124.59 (Ar), 132.47 (Ar), 133.75 (Ar), 137.75 (Ar), 140.25 (Ar), 142.34 (Ar), 144.85 (Ar), 147.33 (Ar).

Elemental analysis calculated for $C_{26}H_{24}N_2O_3S$ (444.15g mol^{-1}): Calcd. (%) C, 70.25; N, 6.30; S, 7.21; H, 5.44. Found: (%) C, 70.27; N, 6.29; S, 7.19; H, 5.45.

2.4. Synthesis of polymers

PEIa-PEId were synthesized via two-step process by reactions of diamine 1B with different dianhydrides (a-d). The synthesis of PEIa is employed as an example to show the general synthetic method employed to prepare the PEIs. A mixture consisting of 1.20 g (2.70 mmol) of diamine 1B, 1.19 g (2.70 mmol) of 6FDA, and 100 mL of NMP were added to a 250-mL, three-necked flask which was equipped with a mechanical stirrer, a condenser, and a nitrogen inlet. The reaction mixture became viscous after 2 h. Then, 50 mL of NMP was added to dilute the solution. The mixture was constantly stirred for 2 h at room temperature to give poly(amic acid) (PAA). In the next step, 16.8 mL of triethylamine in 50 mL of NMP was added slowly to the reaction mixture and it was stirred for another 4 h at room temperature. The inherent viscosity of the PAA**a** was 1.78 dL/g, as measured in DMAc at a concentration of 0.5 g/dL at 30 °C. The PAA was converted into PEI with either a thermal or chemical imidization method. In the thermal imidization method, about 2 g of the PAA solution was spread into a Petri culture dish 7 cm in diameter and baked at 90 °C overnight (ca. 12 h) for the removal of the casting solvent. The semidried PAA film was further dried and converted into the PEI by sequential heating at 150 °C for 30 min, at 200 °C for 30 min, and at 250 °C for 1 h for the elemental analysis, tensile testing, X-ray crystallography and thermal analysis. The PEI films were further heated at 350 °C for another 1 h to ensure the complete imidization. In the chemical imidization method, 5 mL of acetic anhydride and 2 mL of pyridine were added to the remaining PAA solution, and the mixture was heated at 100 °C for1 h to affect a complete imidization. The resultant solution of the polymer was poured slowly into 250 mL of methanol, and the precipitate was washed thoroughly with methanol and hot water, collected by filtration, and dried in air at 150 °C for 4 h. Other polymers were prepared by the similar procedures.

PEIa: FT-IR (KBr, cm^{-1}): 3375 (s, br), 2923 (s), 1783 (w), 1728 (w), 1592 (m), 1525 (m) 1461 (w), 1353 (w), 1250 (w), 1154 (m), 1106 (w), 836 (w), 728 (w), 702 (w), 569 (w).

^{1}H-NMR (500 MHz, DMSO-d_6, ppm): 2.89 (s, 6H, CH), 6.66-6.671 (d, 2H, Ar-H, J= 3.5), 6.97-6.99 (d, 2H, Ar-H, J= 4.5 Hz), 7.28-7.29 (d, 2H, Ar-H, J= 4.50 Hz), 7.46-7.47 (d, 2H, Ar-H, J= 3.5), 7.65 (s, 2H, Ar-H), 7.95 (s, 2H, Ar-H), 8.18-8.19 (d, 2H, Ar-H, J= 4.5 Hz), 8.36-8.37 (d, 2H, Ar-H, J= 3.5).

PEIb: FT-IR (KBr, cm^{-1}): 3370 (s, br), 2930 (s), 1776 (s), 1725 (s), 1590 (m), 1523 (m) 1455 (m), 1350 (m), 1248 (w), 1150 (m), 1104(m), 832 (w), 726 (w), 698 (w), 563 (w).

^{1}H-NMR (500 MHz, DMSO-d_6, ppm): 2.92 (s, 6H, CH), 6.77-6.79 (d, 2H, Ar-H, J= 3.5), 6.88-6.89 (d, 2H, Ar-H, J= 4.5 Hz), 7.28-7.29 (d, 2H, Ar-H, J= 4.5 Hz), 7.56-7.57 (d, 2H, Ar-H, J= 3.5), 7.58 (s, 2H, Ar-H), 8.15 (s, 2H, Ar-H), 8.38-8.39 (d, 2H, Ar-H, J= 4.5 Hz), 8.57-8.58 (d, 2H, Ar-H, J= 3.5).

PEIc: FT-IR (KBr, cm^{-1}): 3373 (s, br), 2927 (s), 1775 (w), 1725 (w), 1590 (m), 1527 (m) 1380 (w), 1151 (w), 1105 (w), 836 (m), 727 (w).

PEId: FT-IR (KBr, cm^{-1}): 3372 (s, br), 2925 (s), 1776 (w), 1725 (w), 1590 (m), 1524 (m) 1352 (w), 1249 (w), 1155 (w), 1105 (m), 728 (w), 562 (w).

2.5. Preparation of the PEI films

A solution of the polymer was made by dissolving about 0.4 g of the PEI sample in 2 mL of NMP. The homogeneous solution was casted onto a glass substrate and heated in oven at 80 ^{o}C for 8 h to remove most of the solvent; then the semi-dried film was further dried in vacuum at 150 ^{o}C for 8 h. The obtained films were around 30 μm thick.

3. Results and discussion

3.1. Preparation and characterization of the diamine monomer

Scheme 1 explains the synthetic method for the ether diamine 1B using a two-step process. In the first step, aromatic nucleophilic displacement of 1-chloro-4-nitrobenzene with 2-(2-hydroxy-5-methylphenylsulfinyl)-4-methylphenol in the presence of K_2CO_3 in DMAc resulted in intermediate dinitro compound. In the second step, this dinitro was reduced to diamine 1B by hydrazine in the presence of Pd/C in ethanol. The chemical structure of the synthesized diamine was proved by elemental analyses (reported in the experimental section), FT-IR, ^{1}H NMR and ^{13}C NMR spectroscopy techniques.

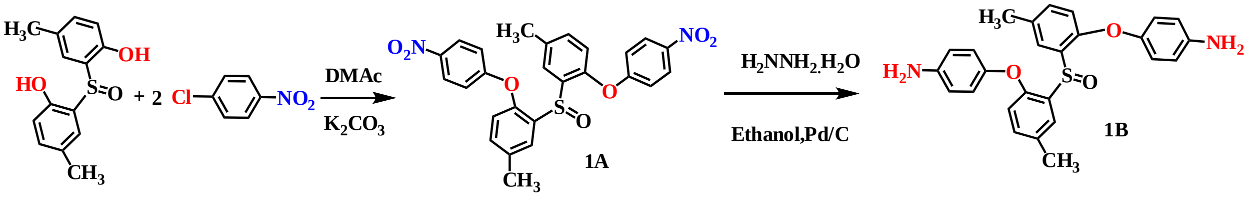

Scheme 1. Preparation of the diamine monomer 1B

FT-IR spectra of the dinitro and diamine are presented in Fig. 1. In the spectrum of the dinitro, the peaks corresponded to the symmetric and asymmetric stretching of –NO_2 groups appeared at 1370 and 1525 cm^{-1}, respectively (Fig. 1a). In the spectrum of diamine (Fig. 1b), characteristic bonds of amino groups at 3447–3383 cm^{-1} (N–H stretching vibrations) and 785 cm^{-}

^{1} (N–H out of plane bending) appeared after reduction and the characteristic absorptions of dinitro groups were disappeared.

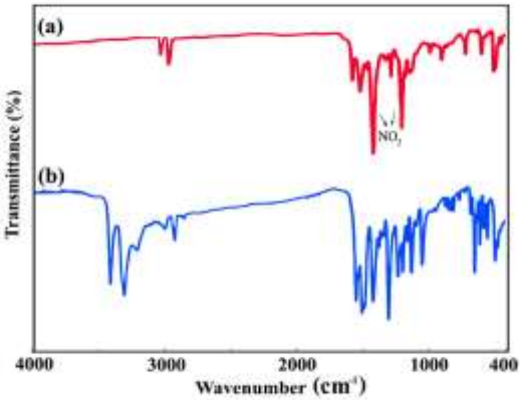

Fig. 1. FT-IR spectrum of the (a) dinitro 1A and (b) diamine 1B.

In the ^{1}H-NMR spectrum of the diamine 1B, the aromatic protons are presented in the range of 6.76-7.62 ppm, and the amino groups are appears at 4.59 ppm. Also the methyl groups are presented at 2.37 ppm (Figs. 2).

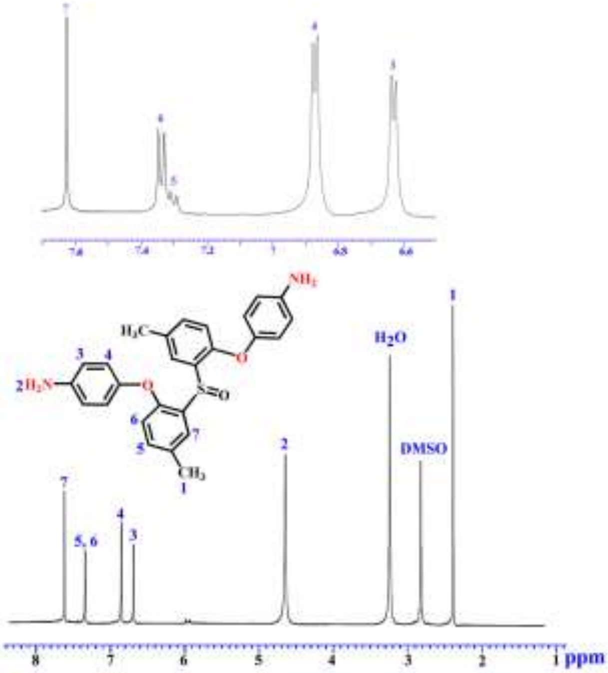

Fig. 2. ^{1}H-NMR (500 MHz) spectrum of diamine 1B in DMSO-d_6 at RT.

Fig. 3 shows the ^{13}C NMR spectrum of the diamine 1B. The aliphatic carbons are presented at 39.55 ppm and the aromatic carbons are presented in the range of 109.11-147.33 ppm (Fig. 3).

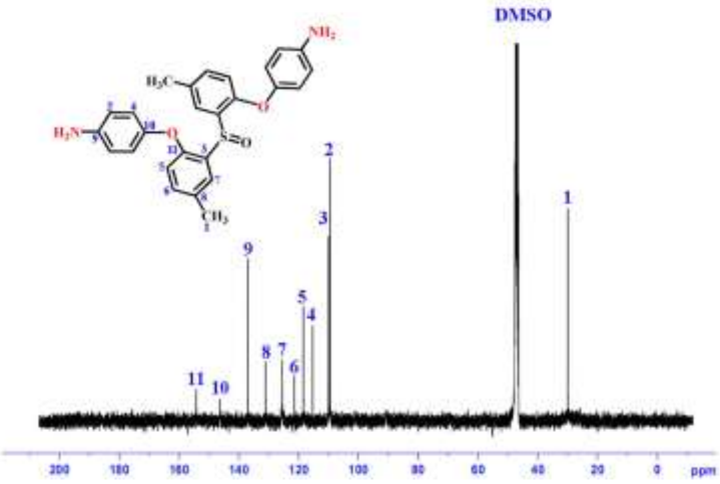

Fig. 3. ^{13}C-NMR (125 MHz) spectrum of diamine 1B in DMSO-d_6 at RT.

3.2. Preparation and characterization of the polymers

The PEIs (a-d) were synthesized from the ether-containing diamine 1B and commercially available dianhydrides (a-d) by a conventional two-step synthetic technique (Scheme 2). The polycondensation reaction was carried out via a two-step procedure: at first, the diamine was reacted with dianhydride at room temperature to produce PAA and then obtained PAA was converted to relate PEIs. Resulting PEIs showed inherent viscosities between 1.09 and 1.93 dL/g at a concentration of 0.5 g dL^{-1} (Table 1). Also, number-average molecular weight (Mn), weight average molar weight (Mw) and polydispersity index (PDI) of the synthesized polymer were further supported by GPC measurements as shown in Table 1. GPC data show that PEIa-PEId have Mn and PDI in the range of 79000-92000 and 1.9-2.1, respectively. Flexible and transparent films of PEIa-PEId could be cast from their solutions conveniently.

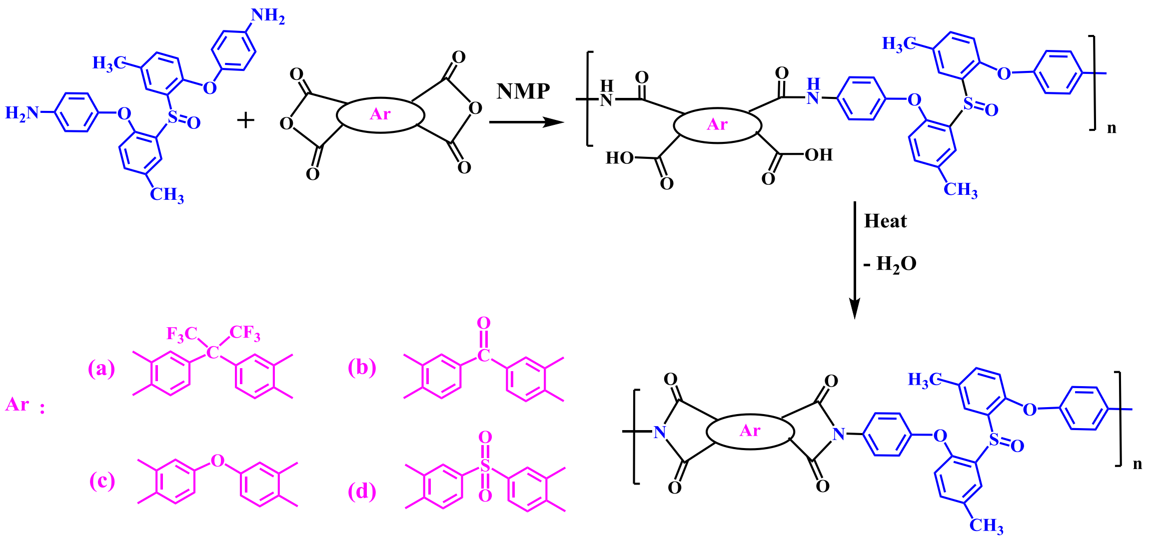

Scheme 2. Synthesis of PAA and PEIs.

Table 1. Molecular weight characterization of the PEIs.

Sample	η_{inh} (dL/g)^a	Mn^b	Mw^c	PDI^d	Film Quality
PEIa	1.78	87250	175410	2.0	Flexible
PEIb	1.46	82354	155720	1.9	Flexible
PEIc	1.09	79560	142600	1.8	Flexible
PEId	1.93	92340	194210	2.1	Flexible

[a] Inherent viscosity of the PEIs precursor measured at a concentration of 0.5 g/dL in DMAc at 30 °C. [b] Mn: Number average molar mass. [c] Mw: Mass average molar mass. [d] Polydispersity index: Mw/Mn.

The conversion of the PAAs to the fully cyclized PEIs was provided by means of FT-IR, ^{1}H NMR spectroscopy and elemental analysis techniques. Fig. 4 show the FT-IR spectra of PAA and PEIa based on 6FDA. The FT-IR spectra of the PEIa showed the characteristic absorption bands of the imide absorption at 1783 (C=O asymmetric stretching), 1728 (C=O symmetric stretching), 1353 (C–N stretching), and 702 cm^{-1} (C=O bending). Also, the peak at 1250 cm^{-1} is corresponded to ether linkage in the polymer structure. The disappearance of bands in the region

2600–3700 cm^{-1} (O–H and N–H stretch) and around 1685cm^{-1} (amide C=O stretch) confirms that PAA was completely conversed into PEIa.

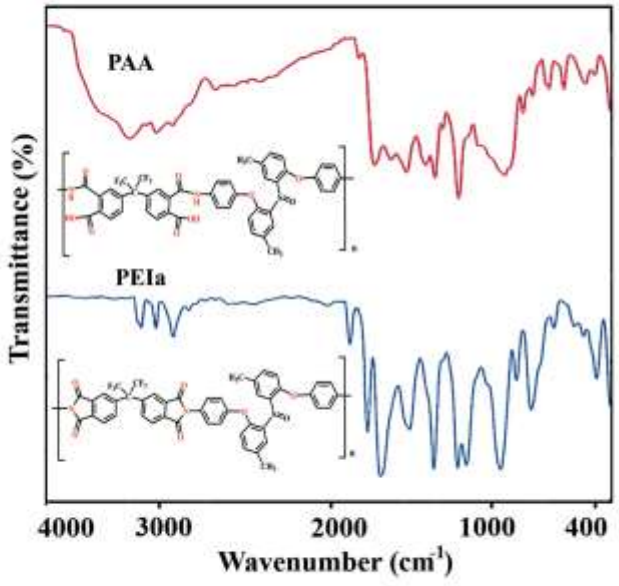

Fig. 4. FT-IR spectrum of the PAA and PEIa based on 6FDA.

Fig. 5 exhibit a typical ^{1}H NMR spectrum of the PEIa based on 6FDA, in which all the peaks have been readily assigned to the hydrogen atoms of the repeating unit and no amide or acid protons at 10-12 ppm appears, indicating that complete imidization was really achieved and PAA film converted into PEI. Also the peaks at around 4.60 ppm corresponding to the amine protons in ^{1}H-NMR spectrum of diamine 1B disappear completely in the ^{1}H NMR spectrum of the polymer (Fig. 5). All PEIs were also recognized by elemental analysis techniques and the results are in good agreement with the calculated ones of the proposed structures (Table 2). These results in sum, confirmed the successful formation of the new PEIs with ether linkages.

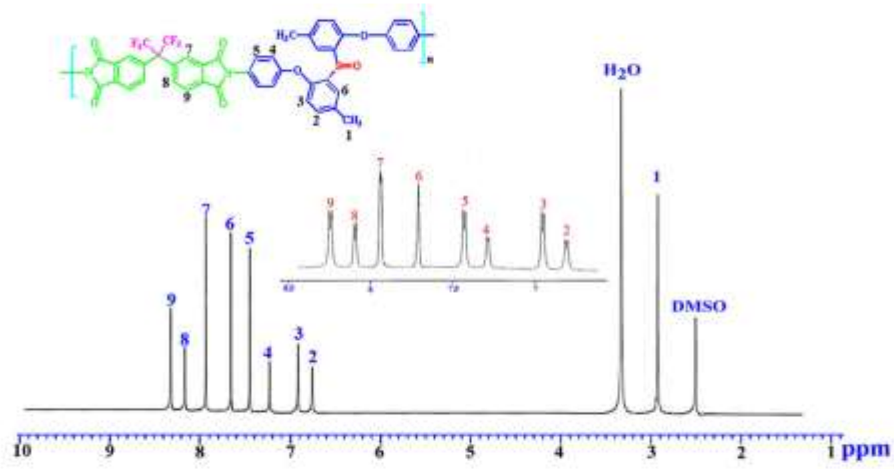

Fig. 5. ^{1}H-NMR (500 MHz) spectrum of PEIa in DMSO-d_6 at RT.

Table 2. Elemental analysis of PEIs (a-d).

Polymer	Formula (Formula weight)	Calculated (%)			Found (%)		
		C	H	N	C	H	N
PEIa	$C_{45}H_{26}F_6O_7N_2S$ (852.12)	63.22	3.48	3.22	62.60	3.86	3.38
PEIb	$C_{43}H_{26}O_8N_2S$ (730.16)	63.23	3.30	3.28	61.32	3.28	3.39
PEIc	$C_{42}H_{26}$ O_8N_2S (718.16)	69.99	3.92	3.89	69.03	3.88	3.87
PEId	$C_{42}H_{28}O_9N_2S_2$ (766.81)	65.61	3.67	3.64	64.98	3.64	3.59

3.3. Solubility behaviors of the PEIs

It is recognized that usual wholly aromatic PIs are insoluble in common organic solvents. To increase the solubility, bulky groups, flexible linkages or noncoplanar structures have been introduced along the polymer chains.[17] It should be noted that good solubility in low-boiling-point solvents is critical for preparing films or coatings at a relatively low processing temperature, which is desirable for advanced microelectronics manufacturing applications. It has been generally known that aromatic ether linkages introduced along the chains of the polymers give a major lower energy of internal rotation.[11] Therefore, the new synthesized PEIs because of flexible linkages in the repeating unit as well as bulky trifluoromethyl groups are soluble in organic solvent. The solubility of the synthesized polymers is summarized in Table 3. According to the Table 3, the resulting polymers displayed good solubility in polar organic solvents such as NMP, DMAc, DMF and DMSO, at room temperature. The solubility varied depending on the dianhydrides used. The flexible ether chain can reduce the rigidity of polymer chain. Also, the presence of bulky CF_3 groups, prevent the close packing of chains in the polymer backbone inhibit close packing and leads to a decreased the interchain interaction to improve solubility.[17,30] Among all polymer, PEIc has good solubility in less polar solvents like chloroform and tetrahydrofuran on heating due to the presence of different flexible ether chain in both diamine and dianhydride monomers.

Table 3. Solubility behavior of the PEIs (a-d).

Polymer	Solubility[a]					
	NMP	DMAc	DMF	DMSO	$CHCl_3$	THF
PEIa	++	++	++	++	-	±
PEIb	++	++	++	++	-	-
PEIc	++	++	++	++	±	±
PEId	±	++	++	±	-	-

[a] Qualitative solubility was tested with 10 mg of a sample (chemically imidized) in 1 mL of the solvent. += soluble at room temperature; ± = soluble on heating; - = insoluble.

3.4. X-ray diffraction of PEIs

The crystallinity of the prepared PEIs was evaluated by XRD method. The XRD patterns of thermally cured PEI films are presented in Fig 6. It was observed that the synthesized PEIs exhibit a broad diffraction peak around 2θ=15-30°, indicating that all polymers are amorphous because of the incorporation of flexible ether groups into the polymer chain. Moreover, the amorphous character is also supported by the reasonable solubility of PEIs, which is in agreement with the general rule that the solubility decreases with increasing crystallinity.[17]

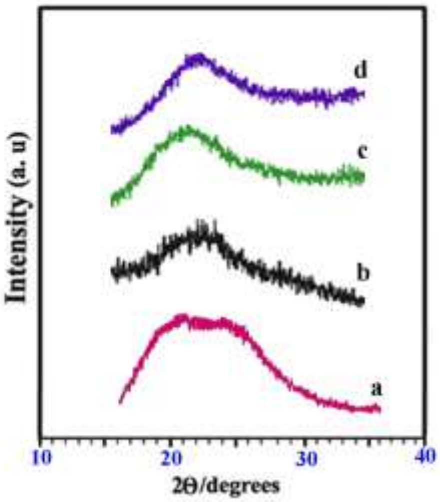

Fig. 6. XRD patterns of PEIa and PEIb.

3.5. Mechanical properties of PEIs

PEI films were subjected to tensile testing and their stress-strain curves were shown in Fig. 7. Table 4 exhibits the mechanical properties of the PEIs, including the tensile strength, tensile modulus, and elongations to break. These films had tensile strength of 118-154 MPa, elongations at breakage of 11-15 %, and tensile module of 2.09-2.28 GPa which shows strong and hard materials. PEIa derived from the aromatic dianhydride 6FDA, shows small tensile strength of 118 which could be attributed to the rigid structure of polymer backbone.

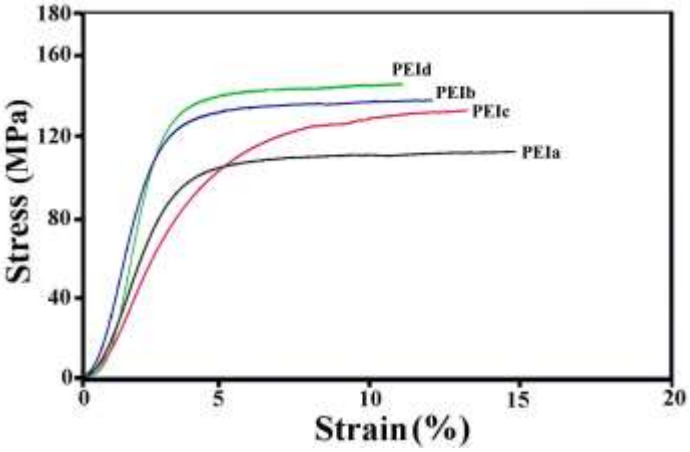

Fig. 7. Tensile stress-strain curves of the synthesized PEI films.

Table 4. Tensile properties of the PEI films

Polymer	Tensile strength (MPa)	Elongation at Break (%)	Tensile modulus (GPa)
PEIa	118	15	2.12
PEIb	144	12	2.09
PEIc	129	13	2.18
PIEd	154	11	2.28

3.6. Thermal properties of PEIs

The thermal stability of the PEIs was evidenced by TGA and DSC and their TGA curves were shown in Fig. 8. TGA results demonstrate that these PEIs are thermally stable: the temperature of 5 % weight loss (T_5) of polymers were in the range of 337–357 °C and 10 % weight loss (T_{10}) values were in the domain of 354-375°C (Table 5). The amount of carbonized residue (char yield or CR) of PIs was from 64 to 71% at 800 °C under a nitrogen gas flow, depending on the structure of dianhydride component. The high char yields of these polymers can be attributed to their high aromatic content.

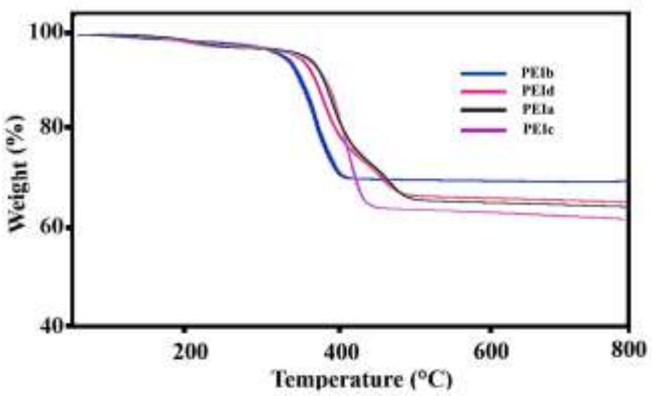

Fig. 8. TGA thermograms of the synthesized PEIs.

Table 5. Thermal characterization of PEIs

Polymer	T_5^a (ºC)	T_{10}^a (ºC)	Char yield (%)^b	T_g^c(°C)
PEIa	356	375	64	303
PEIb	337	354	71	286
PEIc	357	372	62	279
PEId	352	363	66	288

[a] Temperature at which 5 and 10% weight loss was recorded by TGA at a heating rate of 20ºC/min in a nitrogen atmosphere.

[b] Percentage weight of material left undecomposed after TGA analysis at maximum temperature 800ºC in a nitrogen atmosphere.

[c] Measured at a heating rate of 20 ºC/min in a nitrogen atmosphere.

DSC was applied to determine T_g of the PEIs. DSC curves for PEIs (a–d) are reproduced in Fig. 9. The T_g values of the polymers were in the range of 279-303 °C, depending on the structure of diamine or dianhydride monomer and stiffness or rigidity of the macromolecular backbones. So, the enhanced rotational barrier caused by the macromolecular arrangement type increased T_g values.[14] The TGA and DSC results were shown in Table 5. The PEIc based on the

ODPA showed a lower T_g (279 °C) due to the presence of an ether linkage between the phthalimide units.

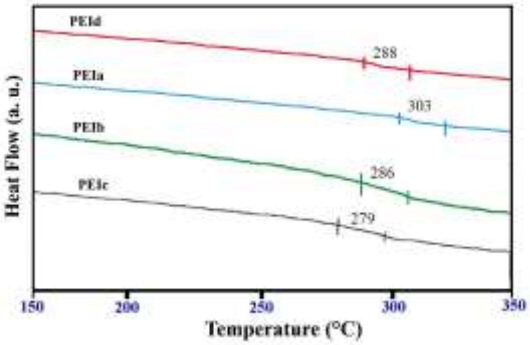

Fig. 9. DSC thermograms of the synthesized PEIs.

3.7. Optical transparency

The optical transparency of the thin films of PEIa and PEIb were measured by UV–vis spectroscopy. To evaluate transparency, the appearance of these films was shown in Fig. 10A. Fig. 10B exhibits the UV-vis transmittance spectra of the PEI films. The cutoff wavelength (absorption edge, λ_0) values and the percentage of transmittance at 500 nm from these spectra were listed in Table 6. The most polymers between the UV and visible area show strong absorption due to the highly conjugated aromatic structures and intermolecular charge-transfer complex formation of PEI.[31] From Fig. 10B, it’s obvious that the PEI films have good optical transparency across the visible light region (450-780 nm). Transparency of PEIa and PEIb films is 89 and 88 %, respectively.

Table 6. Cutoff wavelength (λ_0) from UV–vis spectra of PEIs

Polymer	λ_0[a] (nm)	T_{500}[b] (%)	δ(μm)[c]
PEIa	332	89	37
PEIb	351	88	38

[a] λ_0: Cutoff wavelength of the polymer films.

[b] T_{500}: Transmittance at 500 nm.

[c] δ: The measured thickness of the film samples.

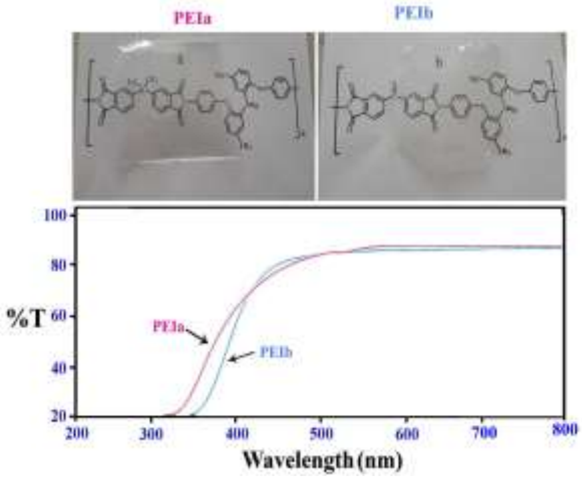

Fig. 10. (A) Visual transparencies of the PEIa and PEIb films and (B) UV-Vis transmittance spectra of PEIa and PEIb films.

3.8. Gas separation performance test

The gas transport properties of the synthesized PEI membranes were measured at 3.5 bar of applied gas pressure and at 35 ^{o}C. The effective permeation area (A) was 5.069 cm^{2}. The membranes were degassed for at least 10 h at 35 ^{o}C within the permeation cell prior to the gas permeation study. To the upstream side of the membranes, the gas pressure (p_i = 3.5 bar) was applied instantaneously and in the downstream side a reservoir of constant volume (119 cm^{3}) was connected with a pressure transducer to observe the total amount of gas which passed through the membranes. The time-lag method was used for the gas transport measurements. This technique allows the determination of mean permeability coefficient (P) from the steady state gas pressure increment $(dp/dt)_s$ in the calibrated volume V of the product standard temperature and pressure (T_0 = 273.15 K, p_0 = 1.026 bar), T is the temperature of measurement, d is the thickness of the membrane and $(dp/dt)_s$ was obtained from the slope of the increments of downstream pressure vs. time plot. The reproducibility of the measurements was better than ± 5% for CO_2

and O_2 permeability measurement but the reproducibility was in the range of ±10% for CH_4 and N_2 permeability measurements. The mean permeability coefficient was determined from Eq. (1):

$$p = \left[\frac{VdT_0}{Ap_i p_0 T} \right] \left(\frac{dp}{dt} \right)_s \qquad (1)$$

Permeability coefficient (P) is a product of diffusivity (D) and solubility coefficient (S). The solubility coefficient S was calculated from Eq. (2):

$$S = \frac{P}{D} \qquad (2)$$

Diffusion coefficient (D) was calculated from the time-lagθ according to Eq. (3):

$$D = \frac{d^2}{6\theta} \qquad (3)$$

The ideal permselectivity of the polymer membranes for a pair of gases A and B is the ratio of the individual permeability and can be expressed from Eq. (4):

$$\alpha_{P(A/B)} = \frac{P_A}{P_B} \qquad (4)$$

Gas transport properties of the four different gases (CO_2, O_2, N_2, CH_4) through these newly synthesized PEIs were studied at 35 ^{o}C under an upstream pressure of 3.5 bar. It is well known that permeability coefficient varies depending on various casting protocols adopted in different laboratories. However, the ideal permselectivity value for a pair of gas can be considered as a standard parameter to compare gas separation performance of a series of polymeric membranes with other polymeric membranes measured in other laboratories.[32] Gas permeability coefficients and permselectivity values of the synthesized polymeric membranes and Kapton as a referenced polymer are presented in Table 7. The diffusion coefficients and solubility coefficient values are shown in Table 8. The solubility selectivity and diffusivity selectivity values have been also depicted in Table 8. Since we could not carry out direct sorption measurements for these polymeric membranes due to limited equipment, definitely, a direct sorption measurement could provide a better insight on the permeation mechanism and more reliable diffusion coefficient values. The diffusion coefficients were determined using the time-lag value of gas flow vs. time plot. We understand that the diffusion coefficient values determined from time-lag values are unreliable when the dual mode transport characteristics apply but within a series of polymers, the measured values of diffusion coefficients can be used for the comparative study of their general behavior.[33]

Table 7 Gas transport characteristics of PEI films.

film	$P(O_2)$	$P(N_2)$	$P(CO_2)$	$P(CH_4)$	$P(O_2)/P(N_2)$	$P(CO_2)/P(CH_4)$	$P(CO_2)/P(O_2)$	$P(CO_2)/P(N_2)$
PI(a)	4.83	0.81	14.31	0.30	5.96	47.70	2.96	17.66
PI(b)	1.95	0.45	8.62	0.22	4.33	39.18	4.42	19.15
PI(c)	0.91	0.24	3.44	0.18	3.79	19.11	3.78	14.33
PI(d)	2.31	0.58	9.71	0.41	3.98	23.68	4.20	14.33
Kapton	0.64	0.11	3.51	0.06	5.82	58.50	5.48	31.91

Permeability coefficient (P) in barrer (1 barrer) 1 cm^3 (STP) cm cm^{-2} s^{-1} $cmHg^{-1}$ $\times 10^{-10}$), measured at 35 °C.

Table 8. Gas diffusion coefficients D×108 (cm^2/s) and solubility coefficients S in 10^{-2} cm^3 (STP)/cm^3 cm Hg of the PEIs at 35 °C and 3.5 bar.

Polymer	CO_2		O_2		$(CO_2)/(CH_4)$		$(O_2)/(N_2)$	
	D	S	D	S	α_D	α_s	α_D	α_s
PEIa	3.22	7.34	10.59	2.01	3.22	11.76	2.06	0.99
PEIb	1.76	3.78	5.25	1.20	2.01	8.56	1.45	1.02
PEIc	1.05	2.66	3.34	0.96	0.78	10.32	0.56	1.65
PEId	2.17	5.22	7.83	1.29	1.12	11.04	1.03	1.72

α_D = diffusivity selectivity values of gas pairs (D_A/D_B). α_S = solubility selectivity values of gas pairs (S_A/S_B).

Fractional free volumes (FFVs) for all the PEI membranes with respect to four different gases were estimated using group contribution method developed by Park and Paul.[34] The order of fractional free volume for the PEI membranes for all the gases was PEIa > PEId > PEIb > PEIc (Table 9). Incorporation of hexafluro linkage in the main chain is known to render loose chain packing, consequently PEIa have higher fractional free volume in the series.[35] The order of gas permeability coefficients of four PEIs membranes for all the gases was PEIa > PEId > PEIb > PEIc. This decreasing trend of permeability coefficient of these polymers (from ‘PEIa’ to ‘PEId’) nicely correlates with their corresponding FFV values for all the gases.[34] The dependence of permeability coefficients with FFV of the PEIs for the four gases (CO_2, O_2, N_2 and CH_4) is represented in Fig. 11. For amorphous polymers, the logarithm of permeability is found to decrease almost linearly with the increasing reciprocal fractional free volume.[35] All the synthesized polymers follow the above trend. For all the PEIs membranes, the gas permeability coefficient follow the order as $P(CO_2)$ >$P(O_2)$ > $P(N_2)$ > $P(CH_4)$ which is basically the reverse order of their kinetic diameter (Å): CO_2 (3.3) < O_2 (3.46) < N_2 (3.64) < CH_4 (3.8). The order of diffusion coefficient for the PEIs followed the order as D(O_2) > D(CO_2) > D(N_2) > D(CH_4). A different order of diffusion coefficients compared to the permeability coefficients order for these four gases can be explained by the fact that there is no or little interaction between O_2, CH_4, and N_2 with the PEIs. However, there is some sort of interaction between CO_2 and PEIs. The interaction is due to the fact that these polymers have imide linkage in chain repeating unit.[36] Permeability of CO_2 through each PEI was higher than the other gases due to the higher solubility coefficient values of CO_2 for each PEI.[37]

Table 9. Fractional free volumes and observed density of the polymers.

Polymer	Density[a]	$(FFV^b)_{CH_4}$	$(FFV^b)_{N2}$	$(FFV^b)_{O2}$	$(FFV^b)_{CO2}$
PEIa	1.44	0.14	0.11	0.12	0.13
PEIb	1.95	0.10	0.08	0.09	0.09
PEIc	2.11	0.08	0.05	0.08	0.07
PEId	1.31	0.12	0.10	0.11	0.11

[a] Density (g/cm^3) measured at 30 ˚C.

[b] FFV = $[V-(V_o)_n]/V$, where V is the volume per mole of the repeat unit of the polymer at 30 ˚C, $(V_o)_n = \sum\gamma_{nk}(V_w)_k$, γ_{nk} is set of empirical factors depending upon gas 'n' and group 'k'. $(V_w)_k$ represents van der Waals volumes for group 'k'.[34]

From Tables 7-9, it can be interpreted that the ideal permselectivities for CO_2/O_2, CO_2/N_2 and CO_2/CH_4 gas pairs are mainly due to the solubility selectivities as diffusivity selectivities are reasonably small.[37,38] Increasing in permeability is generally known to be accompanied with decreased permselectivity, which is consistent with the well-known permeability/selectivity trade off rule common in strongly size-sieving polymers. Robeson demonstrated an upper bound in double logarithmic plots of selectivity against permeability for a wide range of polymers.[5,6] To provide some perspective of the gas separation performance of these PEIs, Robeson plots (double logarithmic plots) of selectivity versus permeability of all the PEIs for O_2/N_2, and CO_2/CH_4 pairs are represented in Fig. 12. The PEIs in this study all fall below the upper bound. Nevertheless, the present PEIs showed improvements in gas-separation performance as proved by their tradeoff points closed to the Robeson' s upper bound as oppose to the conventional polymers like Kapton.

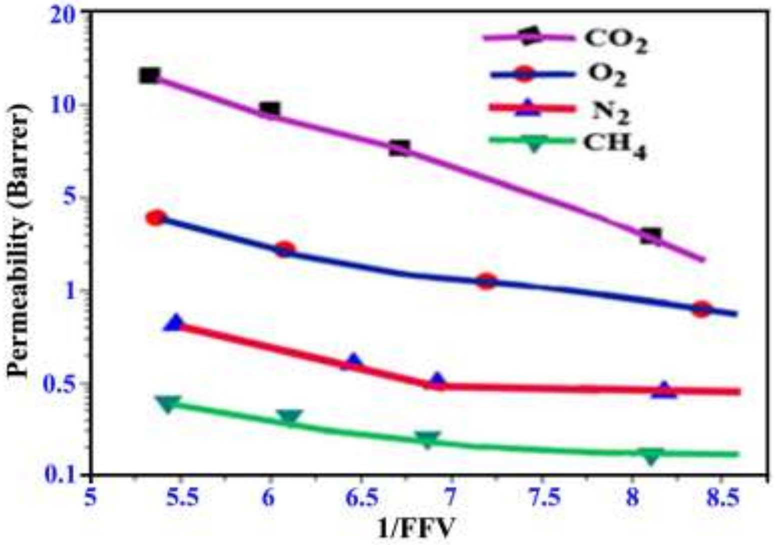

Fig. 11. Representative plots of permeability vs. reciprocal of fractional free volume (FFV) of polymers.

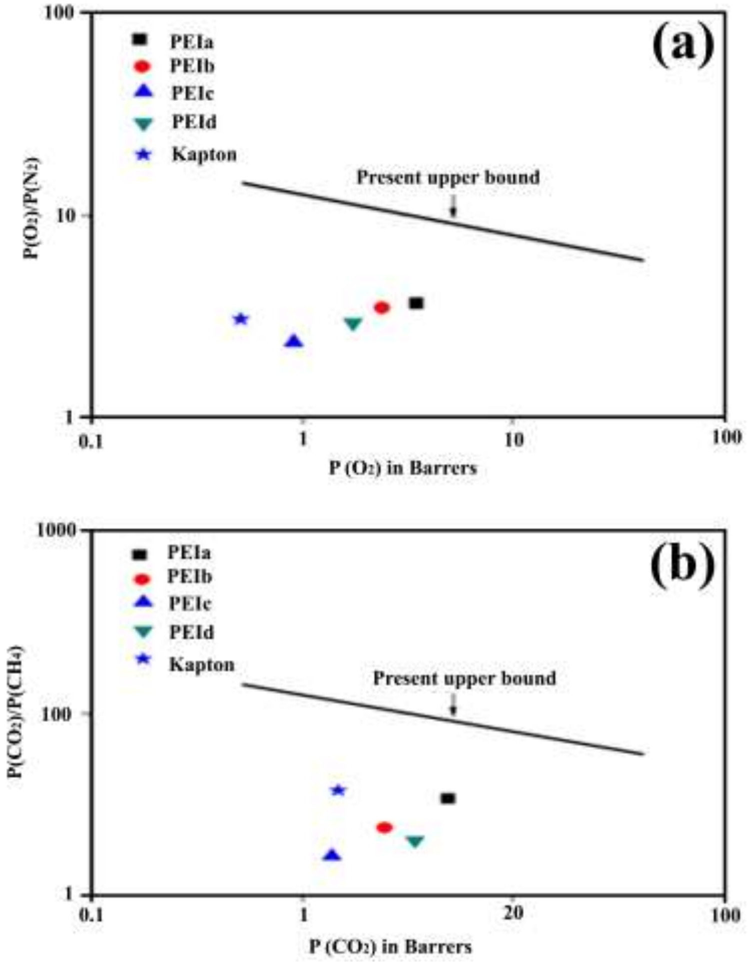

Fig. 12. Robeson plot for a comparison of O_2/N_2 selectivity vs. O_2 permeability coefficients of the PEIs with Kapton.

4. Conclusions

A new aromatic diamine monomer containing ether group was synthesized in two steps. Subsequently, we report the preparation and characterization of new aromatic poly(ether imide)s incorporating flexible linkages which were synthesized by polycondensation reaction between resulting diamine and various aromatic dianhydrides. The complete imidization of polymer was monitored by Fourier transform infrared, proton nuclear magnetic resonance spectroscopy and elemental analysis. The properties of these polymers such as solubility, thermal stability and mechanical resistance were investigated. The introduction of the trifluoromethyl and the flexible ether linkages into the polymer backbone enhanced the solubility of poly(ether imide)s in polar amidic solvents. The resultant polymers show excellent mechanical resistance, thermal stability, and high glass transition temperatures (279–303 °C). According to the UV–Vis spectra theses polymers had good optical transparency in the visible light region. The combination of excellent solubility, film quality, and thermal stability makes these PEIs as potential candidates for high-performance gas separation membrane applications by solution-casting processes. Permeability measurements were made for O_2, H_2, CO_2 and CH_4 at 35 °C. Poly(ether imide)s films showed improvements in gas-separation performance as proved by their tradeoff points closed to the Robeson's upper bound as oppose to the conventional polymers like Kapton.

Acknowledgements

We wish to express our gratitude to the Research Affairs Division Isfahan University of Technology (IUT), Isfahan, for partial financial support. Further financial support from National Elite Foundation (NEF), and Iran Nanotechnology Initiative Council (INIC) is gratefully acknowledged.

References

1 P. M. Budd and N. B. McKeown, *Polym. Chem.*, 2010, **1**, 63-68.

2 Y. Yampolskii, *Macromolecules* 2012, **45**, 3298-3311

3 B. McKeown and P. M. Budd, in Encyclopedia of Membrane Science and Technology, ed. E. M. V. Koek and V. V. Tarabara, John Wiley & Sons, Inc., 2013, vol. 2, p. 781.

4 H. J. Yen, J. H. Wu, Y. H. Huang, W. C. Wang, K. R. Lee, and G. S. Liou, *Polym. Chem.*, 2014, **5**, 4219-4226

5 L. M. Robeson, *J. Membr. Sci.*, 1991, **62**, 165-185

6 L. M. Robeson, *J. Membr. Sci.*, 2008, **320**, 390-400.

7 S. Mallakpour and M. Dinari, *Nano*, 2012, **7** (1250021), 1-10.

8 A. Kausar, S. Zulfiqar, Z. Ahmad, M. I. Sarwar, *Polym. Degrad. Stab.*, 2010, **95**, 2611–2618.

9 M. H. Tsai, Y. Lin, C. J. Chang, P. C. Chiang, J. M. Yeh and et al, *Thin Solid Films* 2009, **517**, 5333-5337.

10 S. Mallakpour and M. Dinari, Prog. *Org. Coat.*, 2012, **75**, 373-378.

11 I. Bacosca, E. Hamciuc, M. Bruma and M. Ignat, *React. Function. Polym.*, 2011, **71**, 905–915.

12 M. Dinari and H. Ahmadizadegan, *RSC Adv.*, 2015, **5**, 8630–8639.

13 G. S. Liou and S. H. Hsiao, *J. Polym. Sci. Part A Polym. Chem.*, 2001, **39**, 1786–1799.

14 M. Dinari and H. Ahmadizadegan. *Polymer* 2014, **55**, 6252-6260.

15 C. H Chang, K. L Wang, J. C Jiang, D. J. Liaw, K. R. Lee, J. Y. Lai and K. H. Lai, *Polymer* 2010, **51**, 4493-4502.

16 T. M. Long, T. MSwager, *J. Am. Chem. Soc.*, 2003, **125**, 14113–14119.

17 M. Dinari and H. Ahmadizadegan. *RSC Adv.*, 2015, **5**, 26040-26050.

18 G. S. Liou and S. H. Hsiao, *Polym. J.*, 2003, **35**, 402-406.

19 M. Hasegawa and K. Horie, *Prog. Polym. Sci.*, 2001, **26**, 259–335.

20 C. P. Yang, Y. Y. Su, S. J. Wen and S. H. Hsiao, *Polymer* 2006, **47**, 7021-7033.

21 L. Tao, H. Yang, J. Liu, L. Fan and S. Yangm, *Polymer* 2009, **50**, 6009–6018.

22 H. Seino, O. Haba, M. Ueda and A. Mochizuki, *Polymer* 1999, **40**, 551–8.

23 C. M. Leu, Y. T. Chang, K. H. Wei, *Chem. Mater.*, 2003, **15**, 3721–3727.

24 X. Zhao, Y. F. Li, X. L. Wang, T. Ma, F. C. Yang, Y. Shao, *J. Polym. Sci. Part A Polym. Chem.*, 2006, **44**, 6836–46.

25 C. Y. Wang, G. Li, J. M. Jiang, *Polymer* 2009, **50**, 1709–16.

26 P. M. Hergenrother, N. T. Wakelyn and S. J. Havens, *J. Polym. Sci. A: Polym. Chem*., 1987, **25**, 1093-1103.

27 C. Liu, L. Li, Z. Liu, M. Guo, L. Jing, B. Liu, Z. Jiang, and et al, *J. Membrane Sci*., 2011, **366**, 73–81.

28 C. P. Yang, Y. Y. Su, S. J. Wen and S. H. Hsiao, *Polymer* 2006, **47**, 7021–7033.

29 X. Zhao, Y. F. Li, S. J. Zhang, Y. Shao and X. L. Wang, *Polymer* 2007, **48**, 5241–5249

30 C. P. Yang and Y. Y. Su, *Eur. Polym. J*., 2005, **41**, 249–258.

31 H. Li, S. Zhang, C. Gong, Y. Liang, Z. Qi and Y. Li, *Eur. Polym. J*., 2014, **54**, 128–137.

32 M. B. Moe, W. J. Koros, H. H. Hoehn and G. R. Husk, *J. Appl. Polym. Sci*., 1988, **36**, 1833–1846.

33 D. R. Paul, *Ber. Bunsenges Phys. Chem*., 1979, **83**, 294–302.

34 J. Y. Park and D.R. Paul, *J. Membr. Sci*., 1997, **125**, 23–39.

35 S. C. Kumbharkar, M. N. Islam, R. A. Potrekar and U. K. Kharul, *Polymer* 2009, **50**, 1403–1413.

36 W. M. Lee, *Polym. Eng. Sci*., 1980, **20**, 65–69.

37 M. D. Guiver, G. P. Robertson, Y. Dai, F. Bilodeau, Y. S. Kang, K. J. Lee, J. Y. Jho and J. Won, *J. Polym. Sci. A: Polym. Chem*., 2002, **40**, 4193–4204.

38 A. C. Puleo, D. R. Paul and S. S. Kelley, *J. Membr. Sci*., 1989, **47**, 301–332.